


## RESEARCH ARTICLE

# Investigation of the influence of pH on the properties and morphology of gelatin hydrogels

K. J. Goudie<sup>1</sup> | S. J. McCreath<sup>2</sup> | J. A. Parkinson<sup>1</sup> | C. M. Davidson<sup>1</sup> |  
J. J. Liggat<sup>1</sup> 

<sup>1</sup>Department of Pure and Applied Chemistry, University of Strathclyde, Glasgow, UK

<sup>2</sup>Terumo Aortic, Inchinnan, UK

## Correspondence

J. J. Liggat, Department of Pure and Applied Chemistry, University of Strathclyde, 295 Cathedral Street, Glasgow, G1 1XL, UK.

Email: [j.j.liggat@strath.ac.uk](mailto:j.j.liggat@strath.ac.uk)

## Funding information

National Manufacturing Institute for Scotland, Grant/Award Number: IDP/012; Terumo Aortic

## Abstract

The behavior of gelatin hydrogels is influenced by the charges located on the amino acid side chains throughout the gelatin molecules. The presence and distribution of ionisable side chains influences the surface activity of gelatin and ultimately determines the material properties. Herein, we report the influence of pH on mechanical properties as studied by texture analysis supported by data from polarimetry, zeta potential, pH titrations and NMR experiments. When adjusted to more extreme pH values (pH 2 and 12), softer gelatin blocks were observed. However, at pH values close to the isoelectric point (pH 5–10), the material is firmer. This behavior is related to the helical content. At pH 2 and pH 12 the surface of the gelatin carries a net charge, positive and negative, respectively, that inhibits the formation of tight helices and lowers the physical crosslink network density. Chemical shift perturbations were observed for the acidic amino acids glutamic and aspartic acid, under acidic pH, where their peaks shifted to higher ppm. Intense amide signals were observed at acidic pH but diminished with increasing pH. This was due to an increase in the rate of chemical exchange between the solvent and peptide amide protons as the pH increases.

## KEYWORDS

gelatin hydrogels, mechanical properties, morphology, polyampholyte

## 1 | INTRODUCTION

Gelatin is one of the most widely used biopolymers with many desirable properties. It is biodegradable, water soluble, non-toxic, biocompatible, inexpensive, non-immunogenic, abundant, easily modified and has good cell adhesion. These characteristics are often tailored and applied in the food, biomedical and pharmaceutical industries.<sup>1–5</sup>

Gelatin is formed by the partial hydrolysis of collagen. Hydrolysis breaks down the secondary and higher bonding interactions between the crosslinked polypeptide chains, resulting in the loss of the collagen's fibrous structure and the production of gelatin. The properties and structure of the resulting gelatin are ultimately determined by the intensity and duration of acid or alkaline pretreatment. Gelatin is formed of three major chain fragments:  $\alpha$ -,  $\beta$ - and  $\gamma$ - chains that vary in length, meaning the protein

This is an open access article under the terms of the [Creative Commons Attribution-NonCommercial-NoDerivs](https://creativecommons.org/licenses/by-nc-nd/4.0/) License, which permits use and distribution in any medium, provided the original work is properly cited, the use is non-commercial and no modifications or adaptations are made.

© 2023 The Authors. *Journal of Polymer Science* published by Wiley Periodicals LLC.

is not monodisperse. Within gelatin chains, there are polar and nonpolar regions with a high glycine, proline and hydroxyproline content and with very little aromatic or sulfur functionalities. The nonpolar regions contain repeating units of Gly-Pro-R where R is a nonpolar amino acid such as hydroxyproline. These nonpolar regions are separated by polar chain segments, which contain little to no proline or hydroxyproline residues (Figure 1).

The distribution of these functional groups influences the material properties. The presence of polar and charged amino acids within gelatin gives it the ability to dissolve in water at temperatures above 30°C. These colloidal solutions can form gels upon cooling. As gelatin solutions cool to approximately 25°C, the molecules aggregate and undergo a conformational change, optimizing their interactions and forming a three-dimensional thermoreversible helical network structure. These network structures are held together by weak non-covalent interactions such as hydrogen bonds, van der Waals, hydrophobic and electrostatic interactions (Figure 2).<sup>1-3,7-11</sup>

The helical network is stabilized by intermolecular hydrogen bonds that orientate perpendicular to the gelatin chains, typically involving direct interaction between C=O and NH groups from neighboring gelatin molecules

or via bridging water molecules. The intermolecular interaction between the carbonyl of glycine and the hydroxyl group of hydroxyproline and the presence of water molecules throughout the network help to stabilize the structure. The high proline and hydroxyproline content throughout the gelatin backbone gives this protein its unique structure. The presence of these groups limits the rotation of the gelatin chains and thus gives the backbone stability in the triple helix conformation. The physical properties of gelatin are determined by the sequence and orientation of the amino acid functionalities throughout the backbone.<sup>4,7,9,10</sup>

Gelatin is naturally polyampholytic meaning it contains a mixture of positive and negative charges throughout the amino acid backbone. The properties of gelatin are dependent on the charge distribution and the presence of polar and nonpolar amino acid side chains. Due to the presence of these ionisable side chains, gelatin is influenced by its surroundings. Changes in pH can influence the surface activity of gelatin molecules, resulting in changes to the material properties.<sup>3,12</sup> The isoelectric point is the pH at which the protein is electrically neutral, that is, the net charge of the protein is zero. At the isoelectric point, the surface charges on the gelatin

FIGURE 1 Chemical structure of the most abundant nonpolar and polar/charged amino acids.<sup>6</sup>

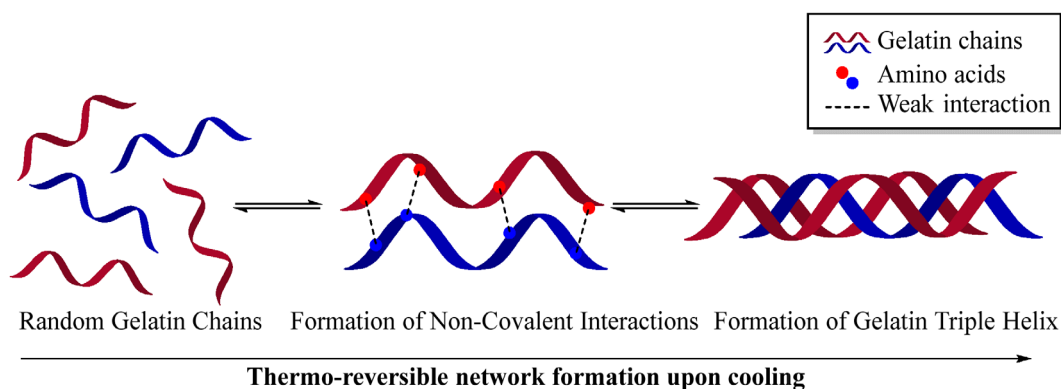
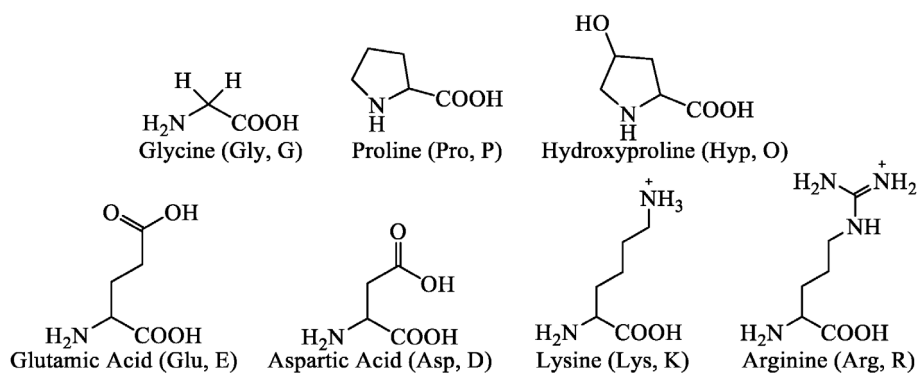


FIGURE 2 Diagram of thermo-reversible gelatin network formation upon cooling. Adapted from Haug and Draget,<sup>1</sup> Schrieber and Gareis<sup>7</sup>

molecules are balanced, minimizing the repulsive forces within the network and allowing the attractive forces to dominate. If the pH of the gelatin is lower than the isoelectric point, then the surface of the gelatin molecules will be positively charged as the different functional groups become protonated and will experience repulsion from other positive charges in the system. Conversely, if the pH of the gelatin is higher than the isoelectric point, then the surface of the gelatin molecules will be negatively charged as the functional groups become deprotonated, meaning the molecules will experience repulsion from other negatively charged chain fragments and ionic species (Figure 3).<sup>7,13–15</sup>

While advantageous, the thermoreversible nature of the gelatin network at relatively low temperatures (25–28°C) limits the application of these hydrogels, particularly for

medical applications.<sup>16</sup> In order to improve the thermal and mechanical properties of these materials chemical crosslinking is often carried out using aldehydes, such as formaldehyde and glutaraldehyde, or by photoinitiation. Crosslinking introduces covalent bonds between the gelatin chains resulting in a stiffer network that is more resistant to thermal and enzymatic degradation.<sup>17</sup> Additionally, different functional groups throughout the gelatin backbone can act as sites for chemical modification. Such amino group (lysine and arginine) modifications can be carried out using reagents such as succinic, methacrylic and carbic anhydride. These modifications improve the material properties, allow the degree of crosslinking to be controlled and introduce photo-crosslinkable moieties.<sup>18–21</sup> However, pH is also an important consideration for these modification and crosslinking reactions. The reaction between amino

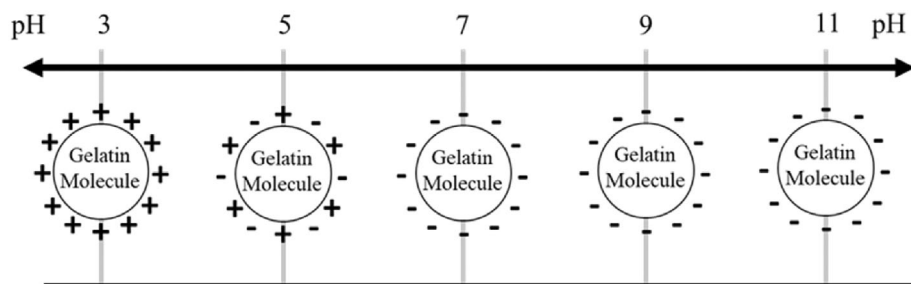
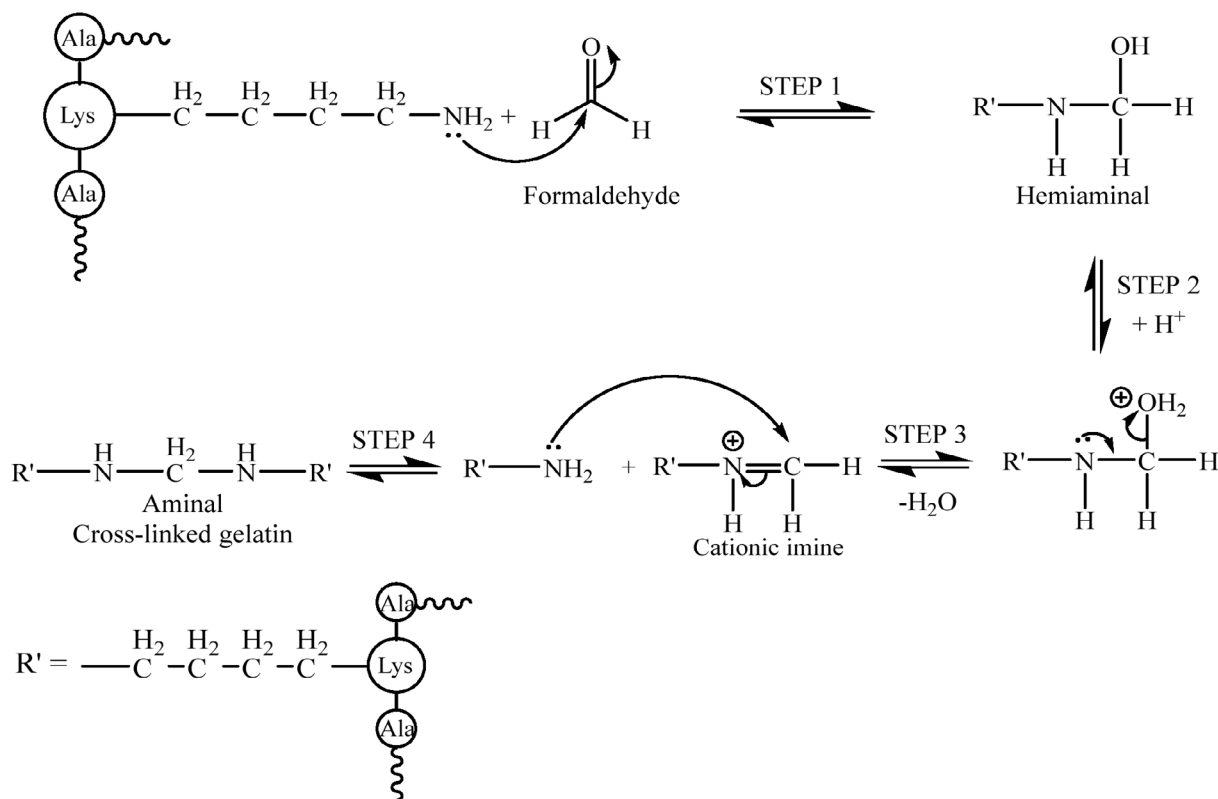


FIGURE 3 Diagram highlighting the surface charge of gelatin molecules as a function of pH.<sup>7</sup>



SCHEME 1 Proposed scheme of chemical crosslinking between amine of lysine and formaldehyde.<sup>22</sup>

acid side chains and anhydrides typically requires pH values  $\geq$  pH 7. Additionally, in the formaldehyde crosslinking mechanism proposed by Digenis et al.<sup>22</sup> (Scheme 1) pH influences the kinetics at various stages of the reaction. The first step of the reaction is the formation of a hemiaminal intermediate and is deemed the rate determining step if the reaction is carried out under acidic conditions. Step 2 is the protonation of the hemiaminal intermediate and is the rate determining step under alkaline conditions. The reaction proceeds with the protonated hemiaminal eliminating water (step 3) and subsequently reacting with an additional free amine group to yield the aminal (crosslinked) product. At low pH values, the process is reversible, meaning the aminal product can be destroyed.

It is therefore critical to understand the influence of pH on molecular morphology as it influences the physical properties of the material. It gives insight into how the protein structure packs, the accessibility of the amino acid side chains for functionalization and crosslinking chemistry and influences the success of these modification reactions.

In this article, we focus on understanding the influence of pH on the material properties and morphology of gelatin hydrogels. This study draws conclusions between the observed material properties and the underlying chemistry that occurs as the pH of the gelatin hydrogels are adjusted from pH 2 to 12. Texture analysis experiments highlight the hydrogel performance at specific pH values. While polarimetry, zeta potential and NMR spectroscopy provide in-depth analysis of changes in molecular ionization at a macroscopic and molecular level. Additional swell testing experiments were carried out to investigate the properties of these gelatin hydrogels (Supporting Information [SI], Section 1). For this testing, samples were set at a different temperature (10°C, experimental constraint) and therefore cannot be directly compared. Despite this difference, the data obtained remains valuable in presenting the overall influence of pH on these hydrogels. This unique combination of analytical techniques provides a comprehensive overview of the pH sensitive nature of gelatin hydrogels, allowing a greater understanding of the material to be developed which is of critical importance for many applications.

## 2 | EXPERIMENTAL

### 2.1 | Materials

The gelatin used for this research was pharmaceutical grade limed bovine bone gelatin with a Bloom value of

250 g and in granule form (8 mesh, ca. 2.36 mm), supplied from the USA by Gelita Inc. A 6.67% solution in water at 60°C has a viscosity of 5.3 mPa and a pH value of 5.57. High bloom gelatin was chosen for this research as Gelita, Inc. state that gelatins with a Bloom value  $>200$  g are widely used in the medical and pharmaceutical industry for hard shell capsules and medical devices.<sup>23</sup>

Bloom strength is the gel strength or the rigidity of a gelatin sample and is analytically measured using a standardized test known as the Bloom test. The test measures the weight (force in grams) required for a specific plunger to depress the surface of a standard thermostatted gel to a defined depth under standard conditions. The gelatin sample must be prepared at a precise concentration (6.67% w/w) in specialized bloom jars.<sup>1,7,24</sup>

For swell testing (SI, Section 1), gelatin samples were crosslinked in methanol stabilized formaldehyde (38/10% v/w) procured from Pioneer Research Chemicals Ltd.

### 2.2 | Gelatin sample preparation

Gelatin samples were all prepared at a total mass: volume concentration of 10 parts per hundred (pph). Typically, 10 g of gelatin was dissolved in 90 mL of deionized water and pH adjusted using 1 molar hydrochloric acid and sodium hydroxide. Once at the correct pH, the solutions were made up to total volume (100 mL) using deionized water, ensuring that despite differences in pH, the concentration of the gelatin solutions remained the same throughout all the testing. The samples were then used immediately or poured into a mold and stored in a Memmert HPP260eco climate chamber overnight (~18 h) before analysis.

### 2.3 | Texture analysis

After setting the gelatin at 20°C for 18 h, the gel was removed from the mold and cut into cylinders with a diameter of 1.5 cm and length of 1 cm. A total of 10 samples were cut per material and returned to the climate chamber and only removed immediately before analysis (Figure 4).

All texture analysis was carried out at room temperature (ca. 20°C) using a Stable Micro Systems TA.XTplus100C texture analyzer fitted with the P/25 25 mm diameter cylinder probe and 5 kg load cell. A pre-programmed test method developed by Stable Micro Systems to investigate the firmness and springiness of gummy confectionary was used to analyze the gelatin samples, measuring the force in compression.<sup>1,25,26</sup> The

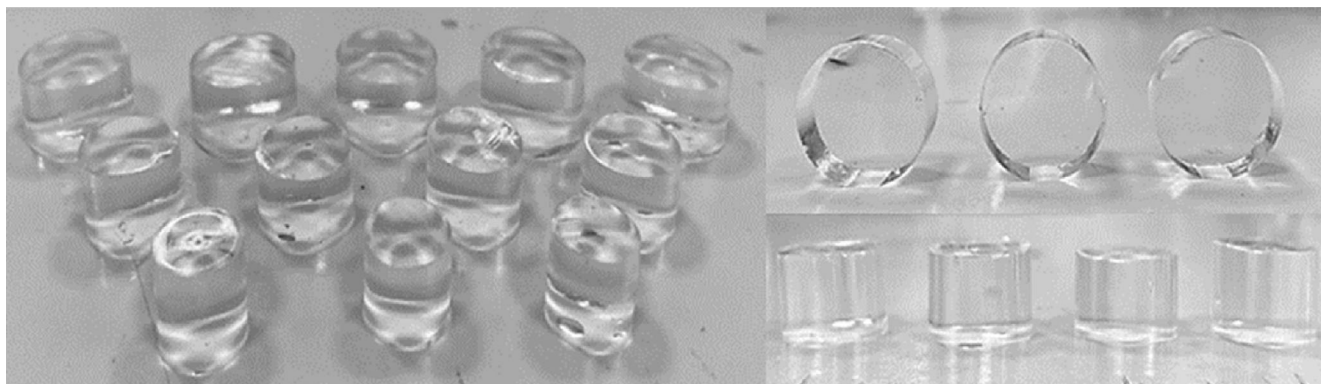


FIGURE 4 Gelatin cylinders used for texture analysis.

test assumes that the surface of the sample is smaller than the diameter of the probe being used. Before analysis was carried out the probe height was calibrated. Once the trigger force of 5 g is attained, the probe proceeds to compress the sample to 20% of its original height. It holds at this distance for 30 seconds and then withdraws from the sample to its starting position, producing a plot of force in grams (or distance) against time in seconds (SI, Figures 3–7). Once the test has been performed, the firmness of the gelatin sample can be calculated by measuring the mean maximum force during the compression. All results were processed using the Stable Micro Systems Exponent Connect software and are presented in the form of average firmness in grams as a function of pH.

## 2.4 | Polarimetry

Gelatin samples were prepared as outlined in Section 2.2. and tested immediately. All polarimetry measurements were carried out using an Anton Paar Modular Circular Polarimeter (MCP 150). The instrument was preheated to 35°C. The sample was allowed to cool at room temperature for 10 minutes before being injected into the polarimeter, after which it was allowed to equilibrate in the probe at 35°C for 10 min. After this time, the measurement was recorded and the temperature of the polarimeter was lowered by 5°C and equilibrated for another 10 min. This process was repeated until all 5°C increments between 35°C and 15°C were recorded. At each temperature, five measurements were recorded and averaged. Each sample was tested in triplicate.

The helical content of gelatin hydrogels can be estimated using the specific rotation values obtained by polarimetry (Equation 1).

Equation 1: Estimation of helical content using specific rotation.

$$X = \frac{[\alpha]_{\lambda} - [\alpha]_{\lambda}^{\text{coil}}}{[\alpha]_{\lambda}^{\text{collagen}} - [\alpha]_{\lambda}^{\text{coil}}}, \quad (1)$$

where  $X$  is the estimated helical content, and its value tends towards zero as the temperature of the solution is increased.  $[\alpha]_{\lambda}$  is the experimentally determined specific rotation of the solution at the wavelength  $\lambda$ ,  $[\alpha]_{\lambda}^{\text{collagen}}$  is the specific rotation of native collagen and  $[\alpha]_{\lambda}^{\text{coil}}$  is the specific rotation of the gelatin in the random coil state. The specific rotation of collagen and coiled gelatin is wavelength dependent when  $\lambda > 300$  nm and can be taken from the literature:

$$[\alpha]_{436}^{\text{coil}} = -256 \pm 5 \quad [\alpha]_{436}^{\text{collagen}} = -800 \pm 10.$$

The specific rotation values for collagen and gelatin are negative due to the left turn/counter clockwise nature of the gelatin helix. These values can be converted to the experimental wavelength ( $\lambda = 589.28$  nm) using the Drude equation (Equation (2)).

Equation (2): Drude equation for calculating specific rotation at a given wavelength.

$$[\alpha]_{\lambda} = D \frac{\lambda_0^2}{\lambda^2 - \lambda_0^2} \quad (2)$$

where  $D$  depends on the conformation of the protein and  $\lambda_0$  is the wavelength of maximum absorption (212 nm).<sup>4,27–30</sup>

## 2.5 | Zeta potential

Gelatin solutions were prepared as outlined in Section 2.2 and tested immediately. All zeta potential measurements were performed using a Malvern



Panalytical Zetasizer Nano ZSP equipped with folded capillary zeta cells at 50°C. The gelatin samples were injected into the zeta cells and equilibrated at 50°C for 2 min before the measurements were recorded. After equilibrating, the instrument recorded five zeta potential measurements for the sample, which were then averaged. Each sample was analyzed in triplicate and the values were then averaged.

## 2.6 | pH titrations

pH titration curves were obtained using a Hanna Instruments HI931 Automatic Potentiometric Titrator. Gelatin solutions were prepared in deionized water at a 10 pph concentration. Once fully solvated the pH was recorded. Typical pH values were approximately pH 5.5. The pH of the gelatin solutions was lowered to approximately pH 1 using 1 M hydrochloric acid (HCl) and titrated against 1 M sodium hydroxide (NaOH) until approximately pH 12 was achieved or a total volume of 100 mL NaOH had been added (instrument limitation). This procedure was carried out in triplicate.

## 2.7 | NMR spectroscopy

Nuclear magnetic resonance spectroscopy was carried out on the different gelatin samples. The gelatin solutions were prepared in deionized water at a concentration of 10 pph and the pH was adjusted using 1 M HCl and 1 M NaOH. Samples were taken from these stock solutions at specific pH values and transferred into NMR tubes for analysis. Sealed capillary tubes containing 30 mM 3-(trimethylsilyl)propionic-2,2,3,3- $d_4$  acid sodium salt (TMSP) in deuterated water were placed inside the NMR tubes as internal reference standards (0 ppm). The NMR tubes were placed in a Dewar flask containing hot water to ensure the samples did not solidify.

1D  $^1\text{H}$  and 2D [ $^1\text{H}$ ,  $^{13}\text{C}$ ] HSQC NMR spectra were acquired on a Bruker AVANCE II+ 600 MHz NMR spectrometer with  $\text{H}_2\text{O}$  solvent suppression using a broadband (BBO-z) probehead equilibrated at a temperature of 50°C. All spectra were processed using the Bruker TopSpin software.

## 3 | RESULTS AND DISCUSSION

### 3.1 | Texture analysis

Texture analysis compression tests were carried out to investigate the influence of pH on the mechanical

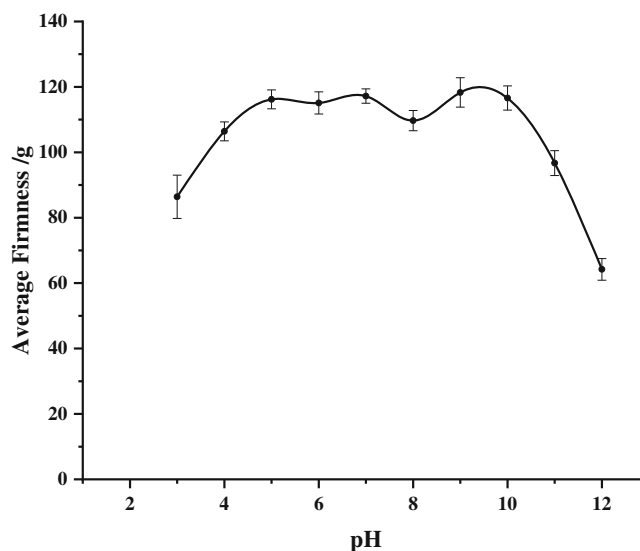


FIGURE 5 Influence of pH on the firmness of gelatin hydrogels.

properties of gelatin hydrogels (SI, Figures 3–7). The data presented in Figure 5 show the average firmness values obtained for gelatin blocks set at different pH values from pH 2 to 12. These compression tests highlight that the firmness of gelatin hydrogels is strongly influenced by varying the setting pH. The softest gels were observed for the samples set at the more extreme pH values tested with firmness values of 86.4 and 64.2 g for samples set at pH 2 and pH 12 respectively. The firmest gelatin blocks were those set between pH 5 and 10, reaching firmness values of ~115 g. On initial inspection, the samples set at pH 8 seem to exhibit slightly softer gels than those set between pH 5 and 10, deviating slightly from the trend. However, it is proposed that this observation is due to experimental variability as the deviation is within experimental error. The overall trend observed was almost the inverse of the data obtained from the swelling experiments outlined in SI, Figure 2. As the gelatin pH deviated from neutral, the gelatin blocks were typically softer and exhibited greater swelling ratios. Despite following a similar trend, it should be noted that the changes observed in the mechanical properties at acidic pH were not as extreme as those seen for the swelling experiments. This correlation supports the hypothesis of changes in functional group ionization throughout the gelatin backbone and its impact on the gelatin network structure.

Similar observations were made by Koli et al.<sup>31</sup> and Choi and Regenstein<sup>32</sup> when studying the influence of pH on the Bloom strength of gelatin from different sources. Bloom strength is a standardized measure of gel strength (g) and can therefore be used to support the data shown in Figure 5. In both studies, all the gelatin materials tested were sensitive to changes in pH. All showed

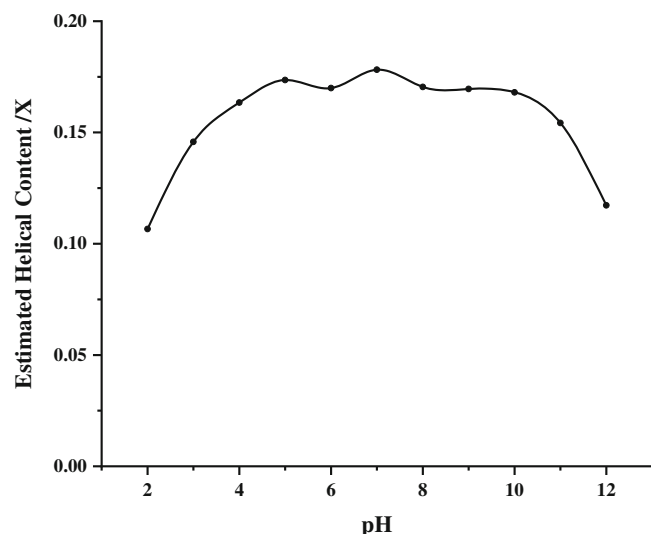


FIGURE 6 Influence of pH on the helical content of gelatin solutions at 20°C.

the highest gel strength when the pH was close to the isoelectric point and the lowest gel strength values as a wider pH range was explored.

It is suggested that there is a relationship between gel strength and the isoelectric point of the material. The attractive and repulsive Coulombic forces between the gelatin chains are dependent on the charge density of the individual chains and can change as a function of pH.<sup>33</sup> At the more extreme acidic and alkaline pH values, the gelatin network experiences substantial repulsive forces that push the gelatin molecules apart, preventing their orientation into an ideal network structure. This causes weaker long-range Coulombic interactions, resulting in the formation of soft hydrogels that require less force to be compressed. When the pH is closer to the isoelectric point of the material, the balanced attractive forces dominate, allowing the gelatin chains to orientate into a more compact configuration. This results in a stiffer gel that requires more force to compress.<sup>34</sup>

### 3.2 | Polarimetry

Polarimetry measurements were carried out to investigate the morphology of the gelatin network and study any changes with pH. The specific rotation across the pH range of pH 2–12 was obtained and the helical content of the material was estimated to develop a greater understanding of material changes at a molecular level and how they lead to the observed changes in mechanical properties. The data displayed in Figure 6 show the estimated helical content of 10 pph gelatin solutions at 20°C across the pH range tested. Figure 6 shows that pH has a

definite influence on the estimated helical content of the material. The least helical content was observed for the samples adjusted to more acidic and alkaline pH values, with values of 0.11 and 0.12 for pH 2 and pH 12, respectively. The greatest estimated helical content was observed for the samples prepared between pH 5 and 10 with values reaching approximately 0.18.

These measurements are consistent with the findings of Takayanagi et al.,<sup>35</sup> where they investigated the effect of concentration and pH on sol–gel transitions of gelatin. The specific rotation was studied over the pH range of pH 3–9, with the greatest optical rotation observed close to the isoelectric point at pH 5. The least specific rotation was observed in the pH 3 and pH 9 samples. They conclude that these observations were due to changes in charge distribution with pH. At the isoelectric point, the positive and negative charges throughout the molecule are balanced, thereby facilitating helix formation. When the pH deviates from the isoelectric point, the optical rotation gradually lessens as the increase in repulsive charges inhibits intermolecular helix formation.

Comparison of Figures 5 and 6 support the hypothesis proposed for the changes observed during mechanical testing. The samples with the least helical content (pH 2 and pH 12) form softer hydrogels and show the greatest average swelling, as they are less able to form a closely packed network. Further evidence was observed in the region of pH 5–10. These samples had the greatest helical content, formed firmer gelatin blocks that required more force to be compressed and exhibited the lowest swelling ratios. Between pH 5 and pH 10, the charges throughout the gelatin network are more balanced, allowing a stronger and more compact network to form.

Polarimetry measurements were carried out on each sample across the pH range of pH 2–12 and temperature range of 15–35°C. Figure 7 shows the average-specific rotation values obtained for gelatin prepared at pH 4 over the full temperature range. It was noted that as the gelatin solution was cooled from 35°C to 15°C, more specific rotation was observed in the sample.

As the gelatin solutions cool, the molecules have less energy and aggregate, forming non-covalent interactions. At low concentrations, these interactions are typically intramolecular, occurring on individual coiled gelatin chains. When the concentration is increased, the number of intermolecular interactions increases due to the proximity of more gelatin chains. As the gelatin solution is cooled there is fast initial helical growth, followed by slow reorganization. The molecules reorganize to optimize their interactions, resulting in more of an equilibrium state with tighter helices that resemble the native collagen helix and secondary structure. This coil-to-helix transition is very slow due to the high peptide-bond

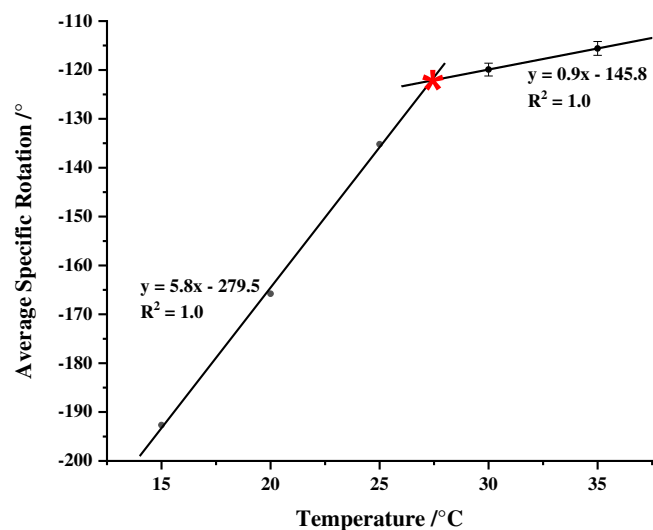


FIGURE 7 Specific rotation of pH 4 gelatin solution over temperature range of 15–35°C. Point of intersection (\*) represents material gelling temperature (27.3°C).

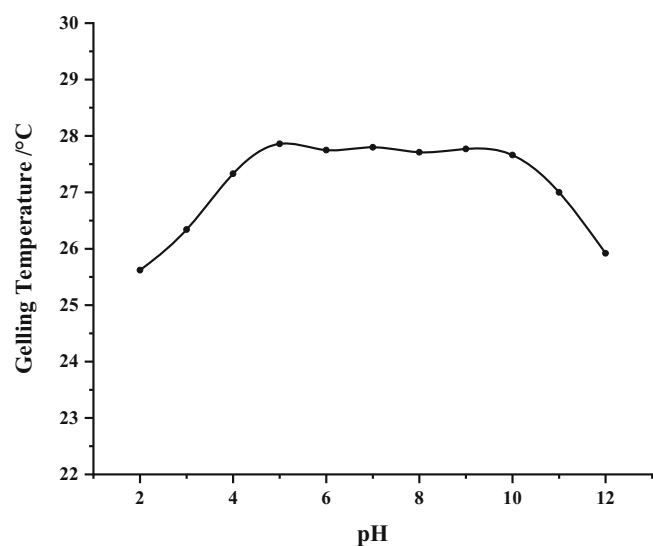


FIGURE 8 Influence of pH on gelatin solution gelling temperature.

content. Djabourov et al.<sup>28</sup> reported that the network does not reach an equilibrium state even after extended annealing times of 100 h. In order to form the triple helix structure these peptide bonds must undergo a high-energy isomerization reaction ( $\sim 72 \text{ kJ mol}^{-1}$ ).<sup>1,4,10,36</sup>

From the data obtained, it was observed that two straight lines could be fitted. One line was fitted to the data in the temperature range of 15–25°C where the gelatin was in the gel state, while the other was fitted to the data in the temperature range of 30–35°C, where the gelatin was in the solution state. The point at which these lines intersect was interpreted as the gelling point of the material, which is 27.3°C for this sample. This result is

consistent with the typical gelling temperature observed by Mad-Ali et al.,<sup>11</sup> where gels were formed between 25°C and 28°C.

This analysis was carried out across the full pH range tested and the gelling temperatures are shown in Figure 8. It was observed that the pH of the material also has an influence on the gelling temperature of the material. Again, the most notable results were those obtained for the more extreme acidic and alkaline conditions.

The gelling temperature of the material is lower at these pH values with gelling temperatures of 25.6°C and 25.9°C for pH 2 and pH 12, respectively. By contrast, the samples pH adjusted to values between pH 5 and pH 10 gelled at higher temperatures in the region of approximately 27.8°C. This is further evidence of changes within the gelatin network as a function of pH. A similar trend was observed by Osorio et al.<sup>37</sup> when studying the influence of concentration, Bloom strength and pH on gelatin melting and gelling temperatures. Higher gelling temperatures were observed for samples adjusted to the isoelectric region of the material (pH 5–10) and lower temperatures were required to gel samples at acidic pH values. The increased repulsive forces within the network at pH values further away from the isoelectric point result in slow helix formation. The system needs to be cooled to lower temperatures to allow molecules to aggregate. However, for the samples whose pH values were adjusted close to the isoelectric point, the positive and negative charges are balanced, facilitating helix formation at higher temperatures.<sup>35</sup>

These polarimetry studies give an insight into the morphology of the gelatin materials at each pH value and support the hypotheses proposed for the changes observed in the material mechanical properties.

### 3.3 | Zeta potential

Zeta potential measurements were carried out to examine the surface charge of the gelatin molecules as a function of pH and to investigate its potential relationship with mechanical testing observations. The data displayed in Figure 9 show the average zeta potential measurements carried out for 10 pph gelatin solutions at 50°C across the pH range of 2–12. The data obtained highlights the change in surface charge of the gelatin molecule as a function of pH. Due to the polyampholytic nature of gelatin, its surface charge is strongly influenced by pH.<sup>38</sup> At acidic pH values, the surface charge of the gelatin molecules is positively charged, reaching +10 mV. This increase in positive charge is a result of functional group protonation. The amino acids throughout gelatin all have pKa values above 3.5. Therefore, it can be assumed that they will all be protonated below this pH, thus leading to



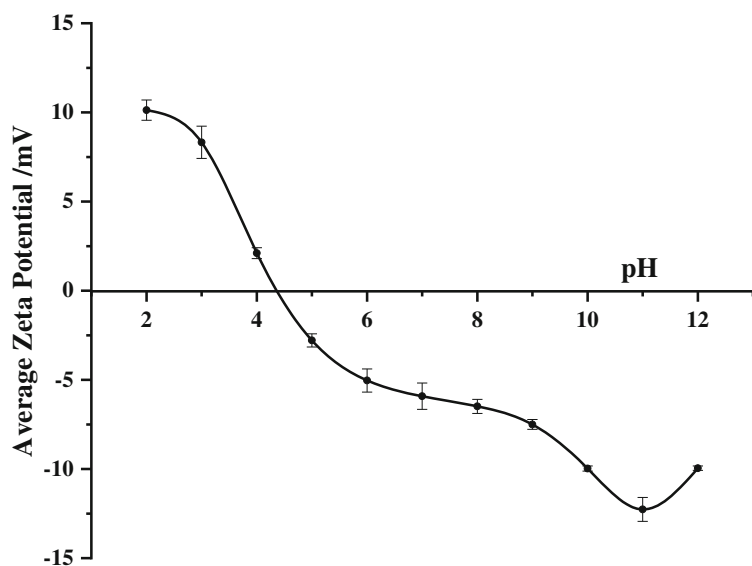


**FIGURE 9** Influence of pH on the zeta potential of gelatin solutions at 50°C. x—intercept represents material isoelectric point (pH 4.4).

increased positive charge. At alkaline pH values, the surface of the gelatin molecules is negatively charged, reaching  $-10$  mV. This negative surface charge is a result of increasing the pH of the solution past the pKa values of the amino acid side chains, thus causing deprotonation and a higher concentration of negative charges.<sup>39</sup>

In a study carried out by Ahsan and Rao,<sup>39</sup> after an initial increase in surface charge with decreasing pH, the surface charge was found to decrease at the lower pH ranges tested (pH 1–3). It was proposed that this was due to an increase in counterions such as  $\text{Cl}^-$ , leading to ion pairing and charge screening effects. This was not observed for our material under acidic conditions. However, it can be seen under alkaline conditions. At pH 12, the surface charge of the material appears to become less negatively charged. Under these conditions, the amino acid side chains are maximally deprotonated. Therefore, increases in pH should not generate positive charge throughout the protein. It is therefore proposed that this decrease in negative charge may be due to the pH adjustment using sodium hydroxide. The presence of excess  $\text{Na}^+$  ions may be interacting with negative chain fragments and shielding negative charges.

The point at which the x axis is intercepted can be interpreted as the isoelectric point of the material, where the positive and negative charges in the network are balanced out.<sup>40</sup> For this material, an isoelectric point of pH 4.4 was observed which is very similar to the isoelectric point determined by Roy et al.<sup>41</sup> for bovine type B gelatin (pH 4.8–5.0). This isoelectric point and surface charge distribution correlates well with the data obtained from mechanical testing and polarimetry measurements. At pH values close to the isoelectric point, the material experiences maximum firmness, minimum swelling and the most helical content. This suggests that the

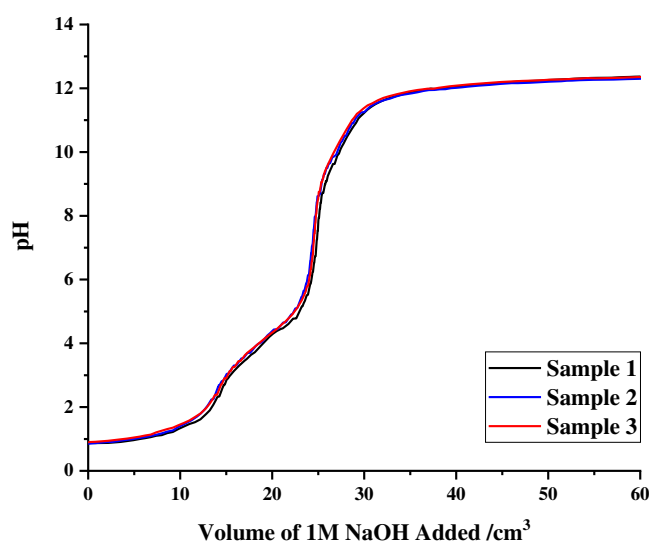


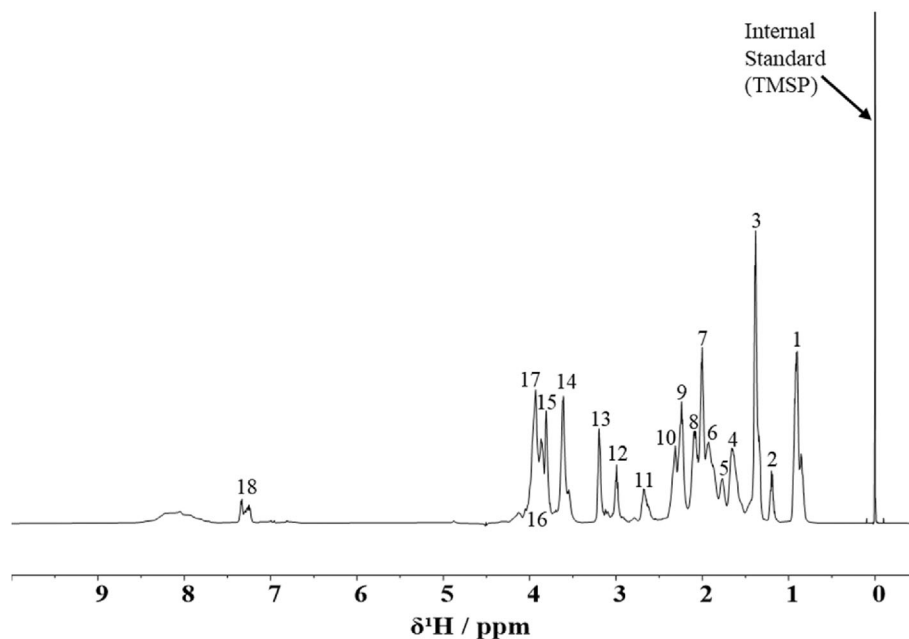
**FIGURE 10** pH titration of gelatin solutions. pH corrected to pH 1 using 1 M hydrochloric acid and titrated against 1 M sodium hydroxide.

interactions within the gelatin network are balanced, resulting in a close and compact structure. At the more acidic and alkaline pH values, where the gelatin molecules are more polycationic and polyanionic, respectively, they exhibit softer gels, display higher degrees of swelling and yield the least helical content.<sup>41</sup> This further supports the observations and hypotheses proposed for the mechanical properties of these hydrogels.

### 3.4 | pH titrations

pH titrations were carried out to study gelatin solutions as a function of pH and identify any pKa values for

**FIGURE 11** Annotated water suppressed 1D  $^1\text{H}$  NMR spectrum of gelatin at pH 7. Numbers correspond to peak assignment in Table 1.



specific amino acid functional groups. Figure 10 shows the titration curves obtained for 10 pph gelatin solutions at 50°C. The solutions were pH corrected to approximately pH 1, using 1 M hydrochloric acid and subsequently titrated against 1 M sodium hydroxide, until around pH 12 was reached.

The titration curves all showed two clear equivalence points. The first equivalence point occurs near pH 3 and the second at close to pH 7. The equivalence point at pH 3 is a result of the deprotonation of acidic amino acids, such as aspartic and glutamic acid, which have pKa values of 3.7 and 4.2, respectively. As of this pH the carboxyl groups of these amino acid side chains are now negatively charged.<sup>42,43</sup>

The sharp equivalence point at pH 7 is a result of the neutralization reaction between the reagents used to alter the pH of the gelatin solutions (HCl and NaOH). This equivalence point was confirmed by blank titrations of 1 M HCl against 1 M NaOH. It is reported throughout the literature that in this pH range, deprotonation of imidazole, imino and  $\alpha$ -amino groups occurs as a result of their pKa values (imidazole pKa 5.5–6.5 and  $\alpha$ -amino pKa 7.5–8.5). These groups are typically present in the amino acid side chains of proline and hydroxyproline. However, due to the large equivalence point from the reagents, no subtle amino acid equivalence points can be observed in this region.<sup>42,44–46</sup>

The titration curves show a slight equivalence point at approximately pH 10.5. It is proposed that this equivalence point is a result of the deprotonation of the  $\epsilon$ -amino acid functionality of lysine, which has a pKa value of 10.3–10.7. In Figure 10 there is no evidence of

deprotonation of guanidino functional groups (arginine) due to the pH range tested. Arginine has a pKa value of approximately pH 12.1 and these experiments do not extend past pH 12.<sup>42–44</sup>

### 3.5 | NMR spectroscopy

Nuclear magnetic resonance (NMR) spectroscopy was carried out to track exact functional group changes with pH. NMR chemical shifts are very sensitive measurements that allow the structure, conformation and chemical environment of proteins to be interpreted. Chemical shift perturbations can occur due to changes in the pH of the system. pH effects the protonation state of the different functional groups throughout proteins and hence influences their ionization. Changes in ionization cause alterations in the electronic environment around the atomic nuclei and result in different extents of shielding, causing chemical shifts to be perturbed from typical values. Chemical shift perturbations can occur through site-specific changes in ionization or through electrostatic interactions that alter the electrostatic field around a nucleus.<sup>47–50</sup> 1D  $^1\text{H}$ ,  $^{13}\text{C}\{-^1\text{H}\}$  and 2D [ $^1\text{H}$ ,  $^{13}\text{C}$ ] HSQC NMR spectroscopy data were used to identify the functional groups responsible for the specific NMR peaks observed and were tracked across the pH range of 2–12. An annotated 1D  $^1\text{H}$  NMR spectrum is shown in Figure 11, where the peak assignment is based on an NMR study by Rodin and Izmailova.<sup>51</sup>

Some of the largest peaks in the spectrum are made up of several small peaks. The small peaks were

TABLE 1 Assignment of peaks observed in  $^1\text{H}$  NMR spectrum of gelatin at pH 7.<sup>51</sup>

$^1\text{H}$ (ppm)	$^{13}\text{C}$ (ppm)	Functional group	Amino acid	% comp	Amino acid summary	Peak number
0.838	13.10	$\delta\text{-CH}_3$	Isoleucine	1.25	Val, Leu, and I-Leu	1
0.910	17.74	$\gamma\text{-CH}_3$	Isoleucine	1.25		
0.929	21.05	$\gamma\text{-CH}_3$	Valine	2.57		
0.857	23.66	$\delta\text{-CH}_3$	Leucine	2.64		
0.909	25.06	$\delta\text{-CH}_3$	Leucine	2.64		
1.198	21.86	$\gamma\text{-CH}_3$	Threonine	1.75	Thre, I-Leu	2
1.198	27.93	$\gamma\text{-CH}_2$	Isoleucine	1.25		
1.382	19.81	$\beta\text{-CH}_3$	Alanine	12.56	Ala, Lys	3
1.393	19.77	$\beta\text{-CH}_3$	Alanine	12.56		
1.412	24.82	$\gamma\text{-CH}_2$	Lysine	3.08		
1.652	27.34	$\gamma\text{-CH}_2$	Arginine	5.41	Arg, Lys	4
1.672	29.35	$\delta\text{-CH}_2$	Lysine	3.08		
1.771	31.10	$\beta\text{-CH}_2$	Arginine	5.41	Arg, Lys	5
			Lysine	3.08		
1.927	31.16	$\beta\text{-CH}_2$	Arginine	5.41	Arg	6
2.001	27.53	$\gamma\text{-CH}_2$	Proline	14.57	Pro	7
2.090	39.98	$\beta\text{-CH}_2$	Hydroxyproline	-	Hypro	8
2.241	36.59	$\gamma\text{-CH}_2$	Glutamic acid	7.82	Glu, Pro	9
2.256	32.34	$\beta\text{-CH}_2$	Proline	14.57		
2.314	39.85	$\beta\text{-CH}_2$	Hydroxyproline	7.82	Hypro, Gln	10
2.381	34.59	$\gamma\text{-CH}_2$	Glutamine			
2.674	41.62	$\beta\text{-CH}_2$	Aspartic acid	4.75	Asp	11
2.992	42.58	$\epsilon\text{-CH}_2$	Lysine	3.08	Lys	12
3.195	43.88	$\delta\text{-CH}_2$	Arginine	5.41	Arg	13
3.613	50.21	$\delta\text{-CH}_2$	Proline	14.57	Pro	14
3.808	58.10	$\delta\text{-CH}_2$	Hydroxyproline	-	Hypro	15
3.867	64.23	$\beta\text{-CH}_2$	Serine	3.45	Ser	16
3.931	45.62	$\alpha\text{-CH}_2$	Glycine	37.78	Gly	17
7.249	132.19	$\delta\text{-CH}_a$	Phenylalanine	1.42	Phen	18
7.296	130.56	$\zeta\text{-CH}_a$	Phenylalanine			
7.332	131.85	$\epsilon\text{-CH}_a$	Phenylalanine			

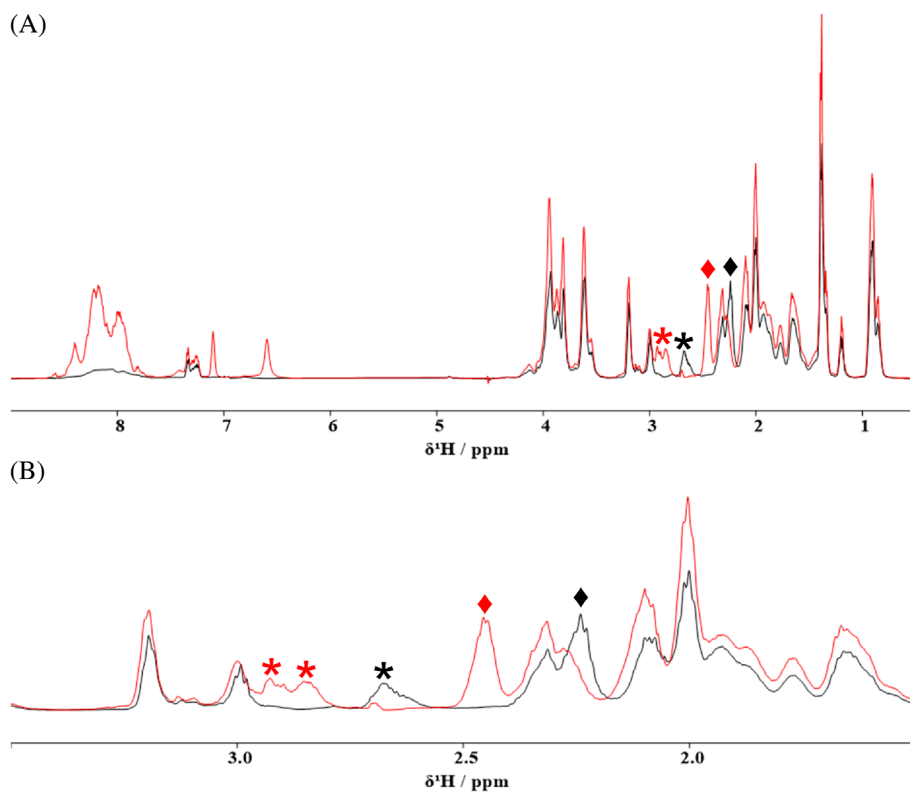
characterized at pH 7, grouped together and have been numbered in Table 1 to simplify analysis. A total of 18 peaks were assigned and tracked as a function of pH to understand how the pH of the solution influences the chemistry of each amino acid throughout the gelatin chain. Understanding the functional group changes at a molecular level can provide insight into gelation interactions at specific pH values.

At pH values below pH 7, peak shifts were observed for the charged amino acids, such as glutamic and aspartic acid. Figure 12A, B highlights the extent of chemical shift perturbations observed in the gelatin

samples at acidic pH. The peak associated with aspartic acid shifts to higher ppm from  $\sim 2.67$  ppm to 2.84 and 2.93 ppm with decreasing pH. At pH 2, 3, and 4, the aspartic acid peaks appear to split into two peaks. According to Rodin and Izmailova,<sup>51</sup> these peaks correspond to  $\beta\text{-CH}_2$  groups. Similar chemical shift changes were observed for the glutamic acid residue peak that moves to higher ppm from  $\sim 2.24$  to  $\sim 2.45$  ppm with acidic pH. Shifting of the glutamic acid peak exposes another peak on the shoulder of the hydroxyproline peak. According to Rodin and Izmailova,<sup>51</sup> this peak corresponds to  $\beta\text{-CH}_2$  of proline, which is present at all

**FIGURE 12** Overlaid water suppressed 1D  $^1\text{H}$  NMR spectra of gelatin at pH 7 (black) and pH 2 (red).

(A) Spectra expanded in the range of interest ( $\delta^1\text{H} = 0.5\text{--}9$  ppm). (B) Spectra expanded in the range of interest ( $\delta^1\text{H} = 1.5\text{--}3.5$  ppm). (\*) highlights the aspartic acid peaks of interest and (♦) highlights the glutamic acid peaks of interest (pH 7 in black and pH 12 in red).



pH values but hidden by glutamic acid peaks at  $\geq$  pH 7.

These chemical shift perturbations occur due to changes in the protonation state of the acidic amino acid groups and can be observed in greater detail in Figure 13A, B. The black contour (pH 7) at  $\delta^1\text{H} \sim 2.68$  ppm/ $\delta^{13}\text{C} \sim 41.5$  ppm (aspartic acid) is not present in the red spectrum (pH 2), it is visible at  $\delta^1\text{H} \sim 2.84$  ppm/ $\delta^{13}\text{C} \sim 38.8$  ppm and  $\sim 2.93$  ppm/ $\delta^{13}\text{C} \sim 38.8$  ppm at acidic pH. Similarly, the black contour at  $\delta^1\text{H} \sim 2.24$  ppm/ $\delta^{13}\text{C} \sim 36.6$  ppm (glutamic acid) is not present in the red spectrum (pH 2), it has shifted and is now visible at  $\delta^1\text{H} \sim 2.45$  ppm/ $\delta^{13}\text{C} \sim 33.1$  ppm at acidic pH. At pH values  $\leq$  pH 4, aspartic and glutamic acid will be protonated due to their respective pKa values of 3.86 and 4.34. This change in charge state alters the electronic environment around the acidic amino acid protons. The proton nuclei become more deshielded as a result of electron density being withdrawn by the new bond formation.<sup>50</sup>

The deshielding effects are consistent with findings from the molecular simulations of Artikis and Brooks<sup>47</sup> and the experiments of Platzer et al.,<sup>50</sup> where chemical shift perturbation of the acidic amino acids due to changes in protonation state were noted, with Artikis and Brooks observing proton chemical shift perturbations with a magnitude  $\Delta\delta(^1\text{H}) = 0.4$  ppm.

Chemical shift perturbation in this pH range also correlates with the data obtained from pH titration experiments (Figure 10). An equivalence point is observed between pH 1.5–4, which encompasses the pKa values for the acidic amino acid residues.

At pH values above pH 7, peak shifts were observed for the basic amino acid residues, particularly lysine. Figure 14A, B highlight the extent of chemical shift perturbations observed in the gelatin samples at basic pH. The peak associated with lysine shifts to low ppm from  $\delta^1\text{H} \sim 2.99$  to 2.58 ppm with increasing pH. According to Rodin and Izmailova,<sup>51</sup> this peak corresponds to the  $\epsilon$ -amino group of lysine.

These chemical shift perturbations occur as a result of changes in the electronic environment around the protons of the lysine residue and can be observed in greater detail in Figure 15A, B. The black contour (pH 7) at  $\delta^1\text{H} \sim 2.99$  ppm/ $\delta^{13}\text{C} \sim 42.5$  ppm (lysine) is not present in the blue spectrum (pH 12), it has shifted and is now visible at  $\delta^1\text{H} \sim 2.58$  ppm/ $\delta^{13}\text{C} \sim 43.8$  ppm under basic pH conditions. At pH values  $\geq$  pH 10.4, lysine is deprotonated due to its pKa value of  $\sim 10.4$ . This deprotonation changes the electronic environment around the amino group of lysine resulting in a residing negative charge. The proton nuclei become more shielded as a result of an increased charge density around the proton.<sup>50</sup> The influence of pH on the rate of chemical exchange at the

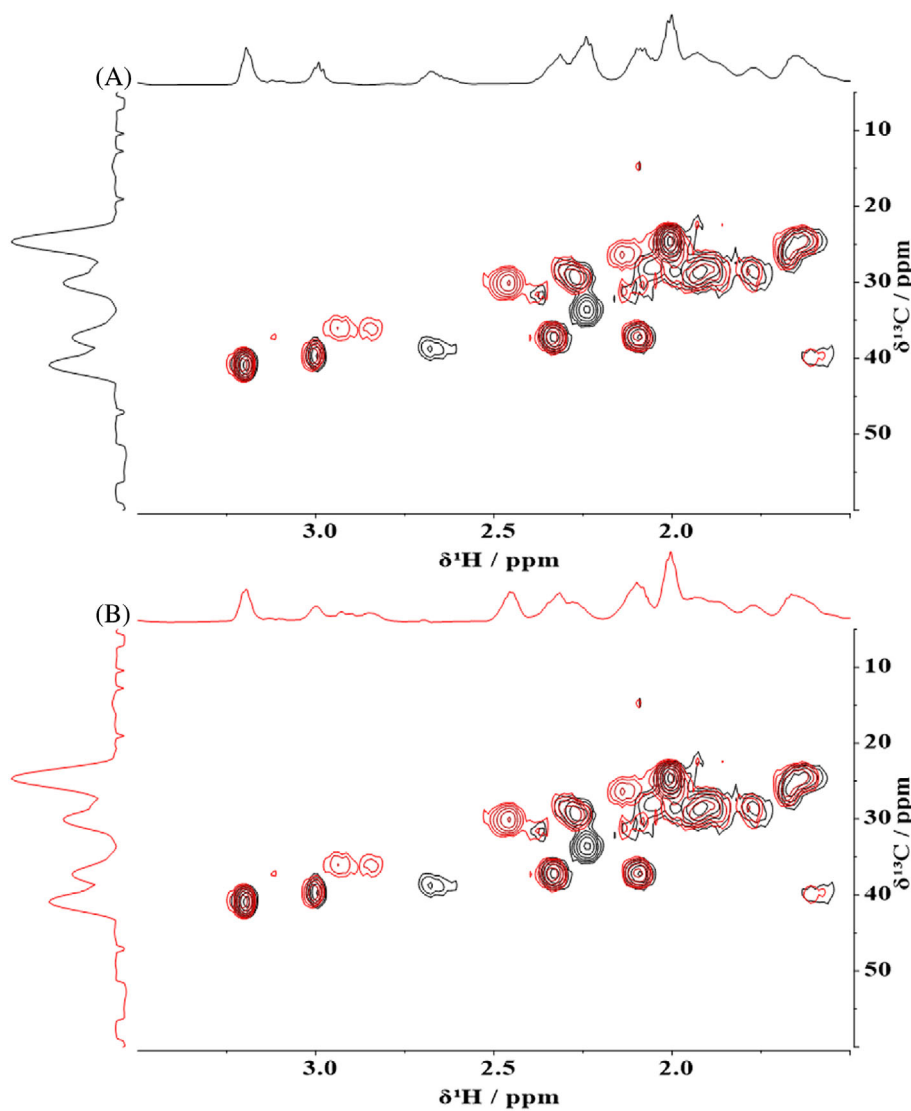


**FIGURE 13** (A) pH 7 (black) and pH 2 (red) 2D [ $^1\text{H}$ ,  $^{13}\text{C}$ ] HSQC NMR spectra of gelatin. The pH 7 1D  $^1\text{H}$  NMR spectrum is displayed as a projection along the F2-axis ( $\delta^1\text{H} = 1.5\text{--}3.5$  ppm) and pH 7  $^{13}\text{C}\{-^1\text{H}\}$  NMR spectrum displayed on the F1-axis ( $\delta^{13}\text{C} = 20\text{--}50$  ppm). (B) pH 7 (black) and pH 2 (red) 2D [ $^1\text{H}$ ,  $^{13}\text{C}$ ] HSQC NMR spectra of gelatin. pH 2  $^1\text{H}$  spectrum displayed on the F2-axis ( $\delta^1\text{H} = 1.5\text{--}3.5$  ppm) and pH 2  $^{13}\text{C}\{-^1\text{H}\}$  NMR spectrum displayed on the F1-axis ( $\delta^{13}\text{C} = 20\text{--}50$  ppm).

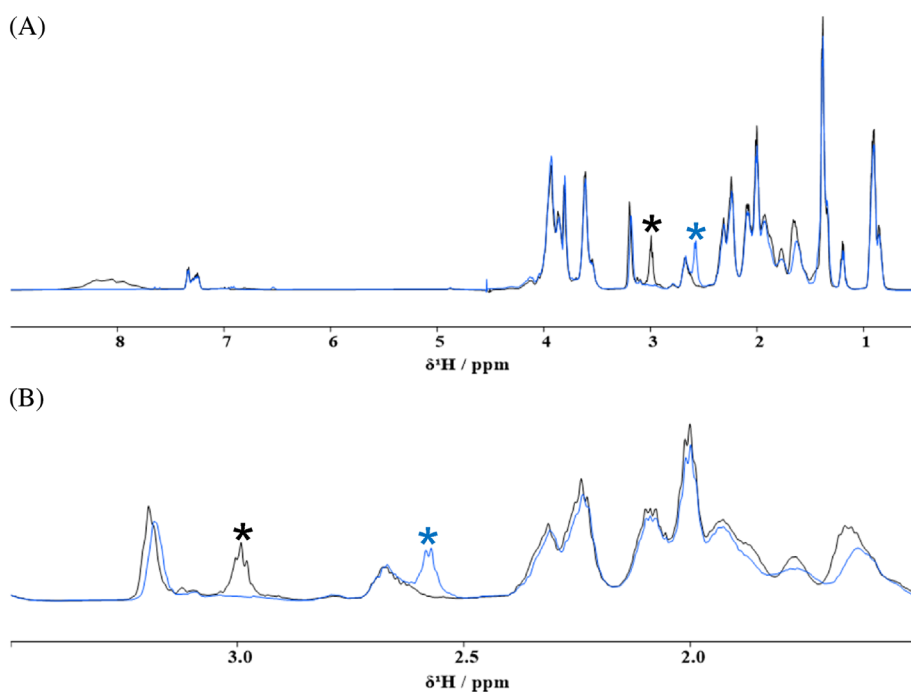


**FIGURE 14** Overlaid water suppressed 1D  $^1\text{H}$  NMR spectra of gelatin at pH 7 (black) and pH 12 (blue). (A) Spectra expanded in the range of interest ( $\delta^1\text{H} = 0.5\text{--}9$  ppm). (B) Spectra expanded in the range of interest ( $\delta^1\text{H} = 1.5\text{--}3.5$  ppm). (\*) highlights the lysine peak of interest (pH 7 in black and pH 12 in blue).



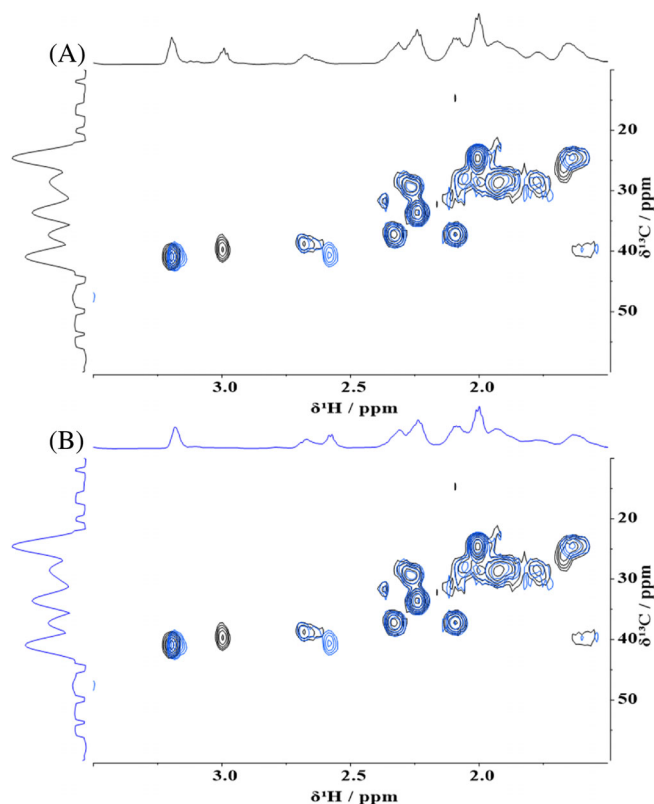
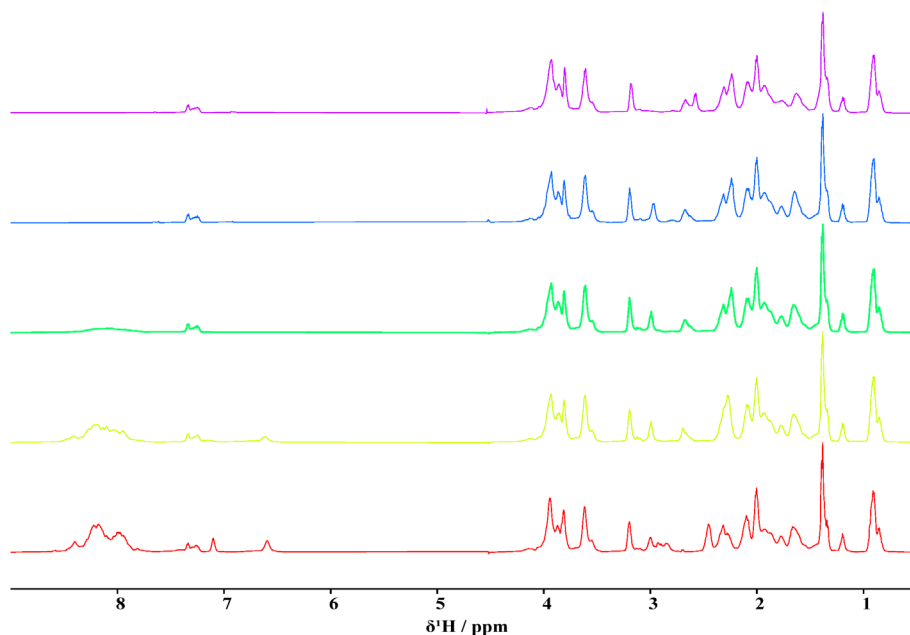


**FIGURE 15** (A) pH 7 (black) and pH 12 (blue) 2D [ $^1\text{H}$ ,  $^{13}\text{C}$ ] HSQC NMR spectra of gelatin. The pH 7 1D  $^1\text{H}$  NMR spectrum is displayed as a projection along the F2-axis ( $\delta^1\text{H} = 1.5\text{--}3.5$  ppm) and pH 7  $^{13}\text{C}\{-^1\text{H}\}$  NMR spectrum displayed on the F1-axis ( $\delta^{13}\text{C} = 20\text{--}50$  ppm). (B) pH 7 (black) and pH 12 (blue) 2D [ $^1\text{H}$ ,  $^{13}\text{C}$ ] HSQC NMR spectra of gelatin. pH 12  $^1\text{H}$  spectrum displayed on the F2-axis ( $\delta^1\text{H} = 1.5\text{--}3.5$  ppm) and pH 12  $^{13}\text{C}\{-^1\text{H}\}$  NMR spectrum displayed on the F1-axis ( $\delta^{13}\text{C} = 20\text{--}50$  ppm).

**FIGURE 16** Offset water suppressed 1D  $^1\text{H}$  NMR spectral comparison of amide peak region of gelatin at different pH values. pH 2 (red), pH 5 (yellow), pH 7 (green), pH 9 (blue) and pH 12 (purple). Spectra expanded into the range of interest ( $\delta^1\text{H} = 0.5\text{--}9$  ppm).



$\epsilon$ -amino group of lysine can be observed in greater detail in supplementary information (SI, Figures 8–10), where the peak is tracked with each increasing pH unit.

The upfield shifting is consistent with the findings from the molecular simulations of Artakis and Brooks<sup>47</sup> and the experiments of Platzner et al.,<sup>50</sup> where they observed chemical shift perturbations of the  $\delta$ - and  $\epsilon$ - amino groups of lysine due to changes in the protonation state.

NMR peak shifts in this pH range also correlate with the data obtained from pH titration experiments (Figure 10). A slight equivalence point was observed at approximately pH 10.5, which corresponds closely to the pKa of the lysine amino acid residue. This analysis, coupled with our zeta potential measurements (Figure 9), provides a more detailed account of the functional group protonation states.

Spectral differences were also observed in the amide proton resonance region ( $\delta^1\text{H} = 7\text{--}9$  ppm) of the  $^1\text{H}$  NMR spectrum, where changes in peak intensity were seen as a function of pH. Figure 16 highlights the difference in peak intensity at various pH values. At neutral pH, the peaks associated with N–H group protons were very weak. However, as the pH decreased, an increase in amide signal response was observed. Conversely, as the pH of the gelatin was increased to basic pH values, the amide signals diminished almost completely.

It is proposed that the change in peak intensity occurs due to a combination of increased rate of chemical exchange and saturation transfer.

Chemical exchange readily occurs between the labile protons of the gelatin amide N–H groups and the solvent

protons. The rate of chemical exchange is dynamic and can be influenced by a number of factors including inductive and steric effects, temperature and pH. This exchange process can be catalyzed by strong acids or bases, with the slowest exchange rates occurring at  $\sim$ pH 2.5. The rate of chemical exchange increases by a factor of 10 per pH unit above or below this minimum (pH 2–3). Changes in rate also influence the line shape observed in an NMR spectrum. When the exchange rate is slow, sharp distinct peaks are observed. As the exchange rate is increased the peaks broaden and begin to coalesce, forming one broad encompassing peak, resulting in the loss of detailed spectral information.<sup>47,52–</sup>

<sup>54</sup> In addition to chemical exchange, the solvent suppression method used can also contribute to diminished peak intensity. Presaturation applies a low power (weak irradiation), continuous pulse to the sample at the solvent resonance for a long period of time (typically 2 s) before the pulse sequence is initiated. This saturation pulse excites all spins that rotate at this frequency (solvent and sample) to the  $x$ – $y$  plane before the  $90^\circ$  pulse is applied. When the  $90^\circ$  pulse is applied these spins are pushed into the  $-z$  orientation where they are not visible to the detector. If the rate of chemical exchange is fast during the saturation pulse timeframe, sample peaks may also be saturated due to saturation transfer.<sup>55–57</sup>

Bundi and Wüthrich<sup>58</sup> observed a similar trend when studying polypeptide chains by  $^1\text{H}$  NMR. In this study, the line intensities of the amide resonances diminished with increasing pH and only the amide protons of the C-terminal residues remained visible at higher pH values. They proposed that this observation was due to an increase in the rate of chemical exchange with the solvent.

The rate of exchange is also influenced by steric hindrance and the electronic environment around the amide protons. The charge density around these protons and their resulting acidity influences the rate at which they can exchange with the solvent. The presence of neighboring polar functional groups inductively withdraws electron density from the amide protons and increases their acidity. This increased acidity results in an increased rate of amide proton removal and a decreased rate of deposition of another proton.<sup>54,59</sup> Similarly, at acidic pH the amide proton nuclei become more deshielded, meaning the amide protons are more tightly bound to the gelatin molecule and less likely to dissociate and participate in chemical exchange resulting in slower exchange rates. In contrast, at neutral to alkaline pH the inverse is observed, with the amide proton nuclei being less deshielded, meaning they are less tightly bound to the gelatin molecule and more likely to dissociate and participate in faster chemical exchange reactions.

## 4 | CONCLUSION

Texture analysis was conducted to study the influence of pH on the mechanical properties of gelatin hydrogels. The gelatin blocks adjusted to more acidic and alkaline pH values (pH 2 and 12), formed softer blocks than those set at pH 5–10. It is believed that these changes with pH are a result of altered electronic environments in the gelatin network. This observation was further highlighted in the data obtained from swell testing experiments (SI, Section 1), where the gelatin blocks set at pH 2 and 12 exhibited a higher degree of swelling than those set in the isoelectric region of pH 5–10. At pH values further from the isoelectric point of the material, there is an increased concentration of like charges. These like charges cause repulsive forces between the gelatin chains, inhibiting the formation of non-covalent interaction and tight helix formation. This leads to a more open network structure with longer range interactions between the gelatin chains, resulting in softer hydrogels that require less force to be compressed. Similarly, the formation of a more open network results in higher degrees of swelling as the water can more easily penetrate the structure.

This hypothesis was investigated further by studying the morphology of the gelatin network as a function of pH using polarimetry, zeta potential, pH titrations and NMR spectroscopy. Polarimetry measurements highlighted that less helical content was observed at pH 2 and pH 12, supporting the hypothesis that the gelatin molecules are not able to pack effectively and cannot form tight helical structures due to opposing charges. Zeta potential highlighted the surface charge of the gelatin molecule as a function of pH, providing an isoelectric point at pH 4.4. At pH values below the isoelectric point, the gelatin was positively charged and above this pH the surface charge was negative. This shows the extent of side chain ionization with pH and validates the changes observed in the material mechanical properties. pH titration and NMR spectroscopy were conducted to study functional group chemical shift perturbations with pH, giving insight into the ionization state of the different amino acids throughout the gelatin backbone at specific pH values. At acidic pH values, the acidic amino acids are protonated resulting in shifting of resonance to high ppm due to the proton nuclei becoming more deshielded. These amino acids, glutamic and aspartic acid, are deprotonated at approximately pH 4, where their peaks move to low ppm. Similarly, the peaks associated with the  $\epsilon$ -amino group of lysine also shift to low ppm when the pH is increased to pH values  $>$ pH 10. This is due to deprotonation of the amino acid side chain, causing the proton to become more shielded due to an increase in local charge density.

Large changes are also observed in the amide proton resonance region as a result of changes in the electronic environment. Intense amide signals are observed at acidic pH but diminish with increasing pH. At acidic pH, these protons are more deshielded, meaning the amide protons are more tightly bound to the gelatin, resulting in intense signals. As the pH is increased, these amide protons become less deshielded, meaning they are less tightly bound to the gelatin molecules and more likely to participate in fast chemical exchange reactions with the solvent. This coupled with saturation transfer results in reduced peak intensity as the pH increases. Combining these techniques has allowed a more detailed understanding of the gelatin network to be developed, providing strong reasoning for the changes observed in the mechanical properties as a function of pH. Additionally, these insights into the gelatin network structure have broadened our knowledge of amino acid ionization and accessibility at specific pH values which is essential for successful site-specific functionalization and crosslinking chemistry.

## ACKNOWLEDGMENTS

KJG thanks Terumo Aortic and the Scottish Research Partnership/ National Manufacturing Institute Scotland for the award of a PhD studentship.

## FUNDING INFORMATION

This work was supported by Terumo Aortic and the Scottish Research Partnership in Engineering/National Manufacturing Institute of Scotland Industry Doctorate Award.

## CONFLICT OF INTEREST STATEMENT

The authors have no relevant financial or non-financial interests to disclose.

## DATA AVAILABILITY STATEMENT

The data required to reproduce these findings are available from the University of Strathclyde Knowledge base research portal here.

## ORCID

J. J. Liggat  <https://orcid.org/0000-0003-4460-5178>

## REFERENCES

- [1] I. J. Haug, K. I. Draget, in *Handbook of Food Proteins* (Eds: G. O. Phillips, P. A. Williams), Woodhead Publishing, Cambridge, UK **2011**, chapter 5, p. 92.
- [2] Q. Xing, K. Yates, C. Vogt, Z. C. Qian, M. C. Frost, F. Zhao, *Scient Rep* **2014**, *4*, 10.
- [3] Z. Jianlong, Q. Congde, L. Weiliang, L. Qinze, *J. Macromolec. Sci. B* **2017**, *56*(10), 739.
- [4] M. Djabourov, J. Leblond, P. Papon, *J. Physique*. **1988**, *49*, 319.
- [5] J. K. Drury, T. R. Ashton, J. D. Cunningham, R. Maini, J. G. Pollock, *Ann. Vasc. Surg.* **1987**, *1*(5), 542.
- [6] R. Bischoff, H. Schlüter, *J. Proteomics* **2012**, *75*(8), 2275.
- [7] R. Schrieber, H. Gareis, *Gelatine Handbook: Theory and Industrial Practice*, WILEY-VCH Verlag GmbH & Co, Weinheim, Germany **2007**, p. 1.
- [8] V. Kumar, D. De, A. N. Gupta, *Int. J. Adv. Res. Sci. Eng.* **2015**, *4*(1), 6.
- [9] K. Nijenhuis, *Thermoreversible Networks: Viscoelastic Properties and Structure of Gels (Advances in Polymer Science)*, 1st ed., Springer Berlin Heidelberg, Berlin, Heidelberg **1997**, p. 267.
- [10] J. L. Gornall, E. M. Terentjev, *Soft Matter* **2008**, *4*(3), 544.
- [11] S. Mad-Ali, S. Benjakul, T. Prodpran, S. Maqsood, *J. Food Sci. Technol.* **2017**, *54*(6), 1646.
- [12] C. Qiao, X. Cao, F. Wang, *Polym. Polym. Compos.* **2012**, *20*(1–2), 53.
- [13] P. Novák, V. Havlíček, in *Proteomic Profiling and Analytical Chemistry*, 2nd ed. (Eds: P. Ciborowski, J. Silberring), Elsevier, Boston **2016**, p. 51.
- [14] A. D. Drozdov, J. deClaville Christiansen, *Int. J. Solids Struct.* **2017**, *110/111*, 192.
- [15] J. Yan, S. Li, G. Chen, C. Ma, D. J. McClements, X. Liu, F. Liu, *Food Hydrocoll.* **2023**, *137*, 108384. <https://doi.org/10.1016/j.foodhyd.2022.108384>
- [16] Z. Muñoz, H. Shih, C.-C. Lin, *Biomater. Sci.* **2014**, *2*(8), 1063.
- [17] P. Dalev, E. Vassileva, J. E. Mark, S. Fakirov, *Biotechnol. Tech.* **1998**, *12*(12), 889.
- [18] N. A. B. Alias, B. O. Omosibi, W. David, N. Huda, *Asia Pacific J. Sustain. Agric. Food Energy* **2017**, *5*, 2.
- [19] T. Liu, G.-F. Zhang, W.-B. Zhou, Z.-G. Su, *Chin. J. Anal. Chem.* **2007**, *35*(1), 43.
- [20] S. Xiao, T. Zhao, J. Wang, C. Wang, J. du, L. Ying, J. Lin, C. Zhang, W. Hu, L. Wang, K. Xu, *Stem Cell Rev. Rep.* **2019**, *15*(5), 664.
- [21] K. S. Lim, B. J. Klotz, G. C. J. Lindberg, F. P. W. Melchels, G. J. Hooper, J. Malda, D. Gawlitta, T. B. F. Woodfield, *Macromol. Biosci.* **2019**, *19*(6), 1900098. <https://doi.org/10.1002/mabi.201900098>
- [22] G. A. Digenis, T. B. Gold, V. P. Shah, *J. Pharm. Sci.* **1994**, *83*(7), 915.
- [23] Gelita. Gelita Pharmaceutical Gelatin – A Multitalented Excipient for Pharmaceutical Applications. Gelita. <https://www.gelita.com/en/applications/pharmaceuticals> (accessed: April 2023).
- [24] C., *United States Pharmacopeial, USP 29, NF 24: the United States Pharmacopeia, the National Formulary, United States Pharmacopeial Convention, North Bethesda, Maryland, USA* **2006**.
- [25] X. Mei, F. M. Etzler, Z. Wang, *Int. J. Pharm.* **2006**, *324*(2), 128.
- [26] P. F. Almeida, S. C. Lannes, *J. Food Process Eng.* **2013**, *36*(6), 824.
- [27] C. Qiao, J. L. Zhang, X. G. Ma, W. L. Liu, Q. Z. Liu, *Int. J. Biol. Macromolec.* **2018**, *107*, 1074.
- [28] M. Djabourov, J. Maquet, H. Theveneau, J. Leblond, P. Papon, *Br. Polym. J.* **1985**, *17*(2), 169.
- [29] L. Guo, R. H. Colby, C. P. Lusignan, T. H. Whitesides, *Macromolecules* **2003**, *36*(26), 9999.
- [30] A. Gogoi, S. Konwer, G.-Y. Zhuo, *Front. Chem. Rev.* **2021**, *8*, 611833.

- [31] J. M. Koli, S. Basu, N. Kannuchamy, V. Gudipati, *Fish Technol.* **2013**, *50*, 126.
- [32] S. S. Choi, J. M. Regenstein, *J. Food Sci.* **2000**, *65*(2), 194.
- [33] J. N. Israelachvili, *Intermolecular and Surface Forces (Intermolecular and Surface Forces)*, 3rd ed., Academic Press, Boston **2011**, p. iii.
- [34] M. Gudmundsson, H. Hafsteinsson, *J. Food Sci.* **1997**, *62*(1), 37.
- [35] S. Takayanagi, T. Ohno, N. Nagatsuka, Y. Okawa, F. Shiba, H. Kobayashi, F. Kawamu, *J. Soc. Photogr. Sci. Technol. Japan* **2002**, *65*(1), 49.
- [36] L. Guo, R. H. Colby, C. P. Lusignan, A. M. Howe, *Macromolecules* **2003**, *36*(26), 10009.
- [37] F. A. Osorio, E. Bilbao, R. Bustos, F. Alvarez, *Int. J. Food Prop.* **2007**, *10*(4), 841.
- [38] N. Pawar, H. Bohidar, *J. Chem. Phys.* **2009**, *131*, 45103.
- [39] S. Ahsan, C. Rao, *Int. J. Nanomed.* **2017**, *12*, 795.
- [40] M. Nagarajan, S. Benjakul, T. Prodpran, P. Songtipya, H. Kishimura, *Food Hydrocoll.* **2012**, *29*(2), 389.
- [41] J. C. Roy, F. Salaün, S. Giraud, A. Ferri, J. Guan, *Carbohydr. Polym.* **2017**, *173*, 202.
- [42] J. H. Bowes, R. H. Kenten, *Biochem. J.* **1948**, *43*(3), 358.
- [43] C. Blei, C. Farrugia, J. Mifsud, E. Sinagra. Potentiometric studies on gelatin solutions and gelatin nanoparticle dispersions, *Proceedings of the 4th World Meeting on Pharmaceutics, Biopharmaceutics and Pharmaceutical Technology*; **2004**. Available from <https://www.um.edu.mt/library/oar/bitstream/123456789/18323/1/OA%20Conference%20paper%20-%20%20POTENTIOMETRIC%20STUDIES%20ON%20GELATIN%20SOLUTIONS%20AND%20GELATIN%20NANOPARTICLE%20DISPERSIONS.1.pdf>
- [44] A. W. Kenchington, A. G. Ward, *Biochem. J.* **1954**, *58*(2), 202.
- [45] Y. Nozaki, C. Tanford, *Methods in Enzymology*, Vol. 11, Academic Press, Cambridge, USA **1967**, p. 715.
- [46] R. L. Thurlkill, G. R. Grimsley, J. M. Scholtz, C. N. Pace, *Protein Sci.* **2006**, *15*(5), 1214.
- [47] E. Artikis, C. L. Brooks 3rd, *Biophys. J.* **2019**, *117*(2), 258.
- [48] M. P. Williamson, in *Modern Magnetic Resonance* (Ed: G. A. Webb), Springer International Publishing, Cham **2018**, p. 995.
- [49] E. R. P. Zuiderweg, *Biochemistry* **2002**, *41*(1), 1.
- [50] G. Platzer, M. Okon, L. P. McIntosh, *J. Biomol. NMR* **2014**, *60*(2), 109.
- [51] V. V. Rodin, V. N. Izmailova, *Colloids Surf. A* **1996**, *106*(2), 95.
- [52] A. D. Bain, in *Encyclopedia of Spectroscopy and Spectrometry*, 3rd ed. (Eds: J. C. Lindon, G. E. Tranter, D. W. Koppenaal), Academic Press, Oxford **2017**, p. 180.
- [53] S. W. Englander, *J. Am. Soc. Mass Spectrom.* **2006**, *17*(11), 1481.
- [54] L. Mayne, in *Methods in Enzymology*, Vol. 566 (Ed: Z. Kelman), Academic Press, Cambridge, USA **2016**, p. 335.
- [55] M. Čuperlović-Culf, in *NMR Metabolomics in Cancer Research* (Ed: M. Čuperlović-Culf), Woodhead Publishing, Cambridge, United Kingdom **2013**, p. 139.
- [56] X. Zhang, M. Liu, X. Mao, in *Encyclopedia of Spectroscopy and Spectrometry*, 3rd ed. (Eds: J. C. Lindon, G. E. Tranter, D. W. Koppenaal), Academic Press, Oxford **2017**, p. 128.
- [57] A. Ross, G. Schlotterbeck, F. Dieterle, H. Senn, in *The Handbook of Metabonomics and Metabolomics* (Eds: J. C. Lindon, J. K. Nicholson, E. Holmes), Elsevier Science B.V, Amsterdam **2007**, p. 55.
- [58] A. Bundi, K. Wüthrich, *FEBS Lett.* **1977**, *77*(1), 11.
- [59] Y. Bai, J. S. Milne, L. Mayne, S. W. Englander, *Proteins* **1993**, *17*, 75.

## SUPPORTING INFORMATION

Additional supporting information can be found online in the Supporting Information section at the end of this article.

**How to cite this article:** K. J. Goudie, S. J. McCreath, J. A. Parkinson, C. M. Davidson, J. J. Liggat, *J. Polym. Sci.* **2023**, *61*(19), 2316. <https://doi.org/10.1002/pol.20230141>